Heliyon 6 (2020) e05756

Contents lists available at ScienceDirect

Heliyon

journal homepage: www.cell.com/heliyon

Research article

Tryptanthrin from microwave-assisted reduction of isatin using solid-state-supported sodium borohydride: DFT calculations, molecular docking and evaluation of its analgesic and anti-inflammatory activity

Craig A. Obafemi [a,*], Oluwaseun B. Adegbite [a], Olatomide A. Fadare [a], Ezekiel O. Iwalewa [b], Nusrat O. Omisore [c], Kayode Sanusi [a], Yusuf Yilmaz [d], Ümit Ceylan [e]

[a] Department of Chemistry, Faculty of Science, Obafemi Awolowo University, Ile-Ife, Nigeria
[b] Department of Pharmacology and Therapeutics, University of Ibadan, Ibadan; Nigeria
[c] Department of Pharmacology, Faculty of Pharmacy, Obafemi Awolowo University, Ile-Ife, Nigeria
[d] NT Vocational School, Gaziantep University, 27310, Gaziantep, Turkey
[e] Department of Medical Services and Techniques, Vocational High School Health Services, Giresun University, 28100, Giresun, Turkey

ARTICLE INFO

Keywords:
Tryptanthrin
Analgesic and anti-inflammatory activity
Isatin
DFT calculations
Molecular docking
Borohydride reduction

ABSTRACT

Tryptanthrin is a potent natural alkaloid with good in vitro pharmacological properties. Herein, we report the synthesis of the compound via a new method involving the reduction of isatin with solid-state-supported sodium borohydride under microwave irradiation. The title compound has been tested for its analgesic and anti-inflammatory activity. The results showed that tryptanthrin dose dependently inhibits oedema and pain formation in all the models used. The agent also exhibited significant higher effects in its anti-inflammatory and analgesic activities better than positive drugs (aspirin and indomethacin) being currently used in the treatment and in the management of acute and chronic forms of pain and inflammatory disorders. The inhibitory potential of the compound was investigated by molecular docking using the software AutoDock Vina. The docking results were used to better rationalize the action and prediction of the binding affinity of tryptanthrin. Density Functional Theory (DFT) calculations at the B3LYP/6-311++G (2df, 2pd) level of theory showed that compared to ascorbic acid, tryptanthrin shows higher antioxidant activity which may be improved upon by functionalizing the aromatic core to enhance its solubility in polar solvents. The calculated electronic and thermodynamic properties obtained for tryptanthrin compete well with the standard ascorbic acid.

1. Introduction

Indolo [2,1-b]quinazoline-6,12-dione (commonly called tryptanthrin) **1** is a natural alkaloid (a weak base) that has been isolated from numerous natural sources including *Couroupita guaianensis* [1, 2], *Strobilanthes cusia* [3, 4], *Polygonum tinctorium* [5, 6], *Isatis tinctoria* [5, 7], *Wrightia tinctoria* [8], *Calanthe discolor* [9], *Phaius mishmensis* [10], *Strobilanthes formosanus* [11]. The orchid *Phaius mishmensis* has also been reported to be rich in carbon-6 substituted-tryptanthrin derivatives [10]. In addition, the alkaloid has been isolated from *Candida lipolytica* microscopic fungi which proliferate when grown in L-tryptophan-containing medium [12] and the marine bacteria *Oceanibulbus indolifex*gen. nov., sp. nov. [13].

Tryptanthrin and its derivatives are of special interest because many of them have been shown to possess an array of biological activities, such as anti-inflammatory (with inhibitory activities against cyclooxygenase (COX)-2, 5-lipoxygenase (LOX), nitric oxide synthase (NOS) and prostaglandin E (2)) [14, 15, 16], antileishmanial [17], antimalarial [18, 19], antimicrobial [20, 21, 22, 23] and antitrypanosomal [24] activities. Also, the compound has been shown to possess antitumor and anti-cancer effects [25, 26, 27, 28].

Tryptanthrin has been synthesized through many different routes, all of which involved the condensation of an anthranilic acid derivative (e.g., benzo[d][1,3]oxazine-2,4-dione, commonly called isatoic anhydride) with an indole derivative (e.g., indole-2,3-dione (isatin) or 1,3-dihydro-2-indolone (oxindole)) (Scheme 1): The reaction of isatin **2** (or an oxindole) with isatoic anhydride **3** is the most common route to

* Corresponding author.
E-mail address: craigobafemi@gmail.com (C.A. Obafemi).

https://doi.org/10.1016/j.heliyon.2020.e05756
Received 25 November 2018; Received in revised form 27 April 2020; Accepted 14 December 2020

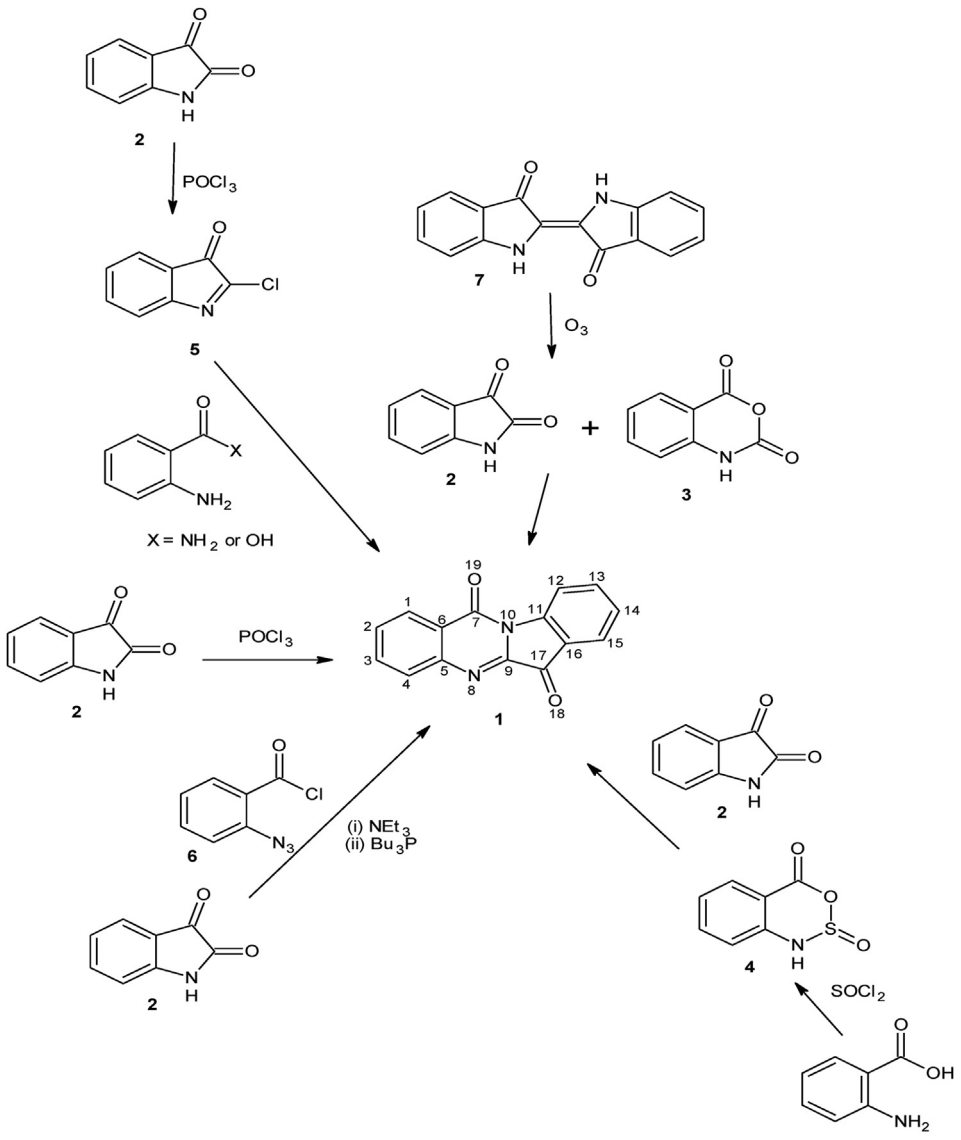

Scheme 1. Synthetic routes to tryptanthrin and its atom numbering.

tryptanthrin [27, 29]. Other methods include the reaction of thionyl chloride with anthranilic acid to give an intermediate 3,2,1-benzoxathiazin-4-one-2-oxide **4**, which reacted further with isatin to afford tryptanthrin in high yield [30], the chlorination of isatin with phosphorus oxychloride (or phosphorus pentachloride) to give 2-chloro-3-indolone **5,** which upon further reaction with anthranilamide (or anthranilic acid) produced tryptanthrin in very high yield [19, 31, 32], reaction of phosphorus oxychloride with excess of isatin [33], a 3-component reaction of isatin with 2-azidobenzoyl chloride **6** and tributylphosphine to give **1** in about 40 % yield via an intramolecular aza-Wittig reaction [34] and ozonolysis of indigo **7** to give **2** and **3,** which then underwent condensation to give tryptanthrin **1** in low yield [35] (Scheme 1).

The present paper reports a new route to synthesis of tryptanthrin using a one-step process of isatin reduction. The product was assessed for its analgesic and anti-inflammatory effects.

Improved understanding to the quantitative structure activity relationship (QSAR) and electronic properties of compounds and their interaction with biological systems is provided by computational theory methods (DFT). Hence, we have performed a DFT study of the compound in both the gas and aqueous phases. In addition, the compound was docked into the binding site of 1CX2 (cyclooxygenase 2) and its binding energy calculated.

2. Experimental

2.1. General

Isatin was purchased from Merck company, while silica, alumina, acetic anhydride and the solvents used (of analytical grade) were purchased from BDH Chemicals Ltd and used without further purification. The melting point of the product was determined on a Gallenkamp (variable heater) melting point apparatus in open capillary tube and is uncorrected. The Infrared (IR) spectrum was recorded on a Buck FTIR spectrophotometer using KBr pellet, while ^{1}H and ^{13}C Nuclear magnetic resonance (NMR) spectra of the pure compound in $CDCl_3$ were recorded on Bruker AMX spectrometer (400 MHz for ^{1}H-NMR, 100 MHz for ^{13}C-NMR, delta in ppm relative to Me_4Si).

Elemental analysis of the compound (C, H, N) was performed on a Carlo Erba-1108 elemental analyzer. Result was within acceptable % of the theoretical value. Electron impact mass spectrum (EI-MS) was obtained on a VG 7070 spectrometer at the inter-departmental centre for mass spectrometry of the University of Trieste.

The progress of the chemical reaction and the purity of the reaction product (title compound) were monitored and determined with the use of silica gel G thin layer chromatography (TLC) plates, in solvent system of

toluene:ethyl acetate (5:2 v/v). The spots on TLC chromatograms were detected with UV light.

2.2. Synthesis

2.2.1. Typical procedure for synthesis of tryptanthrin **1** from isatin

A mixture of isatin (1.0 g, 6.8 mmol), sodium borohydride (0.60 g, 15.9 mmol) and silica (5.0 g) was ground in a mortar to a fine powder and transferred into a beaker, with a glass cover. The mixture was irradiated in a domestic microwave oven (with an emitted power of 400 W) for the required length of time as shown in Table 1 and monitored by TLC (toluene:ethyl acetate, 5:2). A silica gel column (toluene) was used to separate the products to give yellow crystals (0.252 g, 30 %); m.p. 266–267 °C; R_f = 0.90 (EtOAc/toluene, 2:5). IR (υ_{max}, cm^{-1}): 1727 (C=O), 1685 (C=O), 1594 (C=C), 1314, 1113w, 1040w, 755. ^{1}H NMR (400 MHz, $CDCl_3$): δ = 8.60 (d, 1H, J = 8.05 Hz), 8.42 (dd, 1H, J = 1.46, J = 7.87 Hz), 8.00 (d, 1H, J = 8.05 Hz), 7.91 (d, 1H, J = 7.69 Hz), 7.84 (dt, 1H, J = 1.45, J = 7.30 Hz), 7.77 (dt, 1H, J = 1.46, J = 8.05 Hz), 7.66 (dt, 1H, J = 1.09, J = 7.51 Hz), 7.41 (d, 1H, J = 8.05 Hz) ppm. ^{13}C NMR (100 MHz, $CDCl_3$): δ = 182.6, 158.1, 146.6, 146.3, 144.3, 138.3, 135.1, 130.7, 130.3, 127.5, 127.2, 125.4, 123,7, 121.9, 118.0 ppm. The spectra matched with those previously published [19]. MS (EI): m/z = 248 [M]+.

2.2.2. Synthesis of N-acetylisatin **2′b** from isatin

Isatin (2.0 g, 13.6 mmol) was added to acetic anhydride (30 mL) and heated with continuous stirring at 85–90 °C for three hours. The product was obtained either by pouring the cooled reaction mixture into cold water (200 mL) to give a yellow powder (1.66 g, m.p. 135–138 °C) or putting the cooled reaction mixture in a fridge for 12 h to give 1-acetylisatin as yellow crystals (1.50 g, 56 % yield), m.p. = 134–136 °C (Lit [36]. 137–139 °C.).

2.3. Biological screening

The synthesized tryptanthrin was screened for its anti-inflammatory and analgesic properties in experimental albino mice.

2.4. Animals

Albino mice of both sexes (20–26 g) were used. The animals were well cared for (under standard laboratory conditions): bred well and housed in a clean, correctly lit and aerated room in the Animal House, Department of Pharmacology, Faculty of Pharmacy, Obafemi Awolowo University, Ile-Ife. The animals were provided free access to standard commercial diet (Vital Feeds Ltd, Nigeria) and water ad libitum. The experimental procedures were approved by the Obafemi Awolowo University Ile-Ife-Animal Care and Use Research Ethics Committee (OAUI-ACUREC/App/12/2016/01) and performed in accordance with the National institutes of Health (NIH) Guideline for the Care and Use of Laboratory Animals (Publication No. 85-23, revised 1985). Also used is the guideline from Guide for the Care and Use of Laboratory Animals, 8th edition National Research Council (US) Committee for the Update of the Guide for the Care and Use of Laboratory Animals, Washington (DC): National Academies Press (US); 2011.

2.4.1. Anti-inflammatory activity

2.4.1.1. Acute inflammation. The model of acute inflammation used was Carrageenan-induced paw oedema in mice. Animals in the test group (n = 5) were treated with tryptanthrin (6, 12 and 24 mg/kg i.p) or indomethacin (10 mg/kg i.p), while control group mice received DMSO (0.3 mL/kg i.p) treatment only. After one hour of the administration of the compound and standard drug, a solution of 1% carrageenan (0.1 mL) was injected into the plantar surface of the right hind paws of the mice. Two hours after carrageenan injection, the mice were anaesthetized in a jar using a chloroform-soaked cotton wool, and both the right and left hind limbs were cut identically at the ankle joint and weighed.

The amount of oedema developed in the right hind limbs were deduced by the differences in weight [37].

Percentage inhibition was estimated by:

$$\text{Percentage inhibition} = \frac{\{(\text{acute inflammation})\text{control} - (\text{acute inflammation})\text{treated}\}\ \text{X}\ 100}{(\text{acute inflammation})\text{control}}$$

2.4.1.2. Carrageenin-induced pleurisy in mice/pulmonary oedema. A modified procedure described in detail by Vinegar and co-workers [38] and cited by Badilla and others [39] was used in these experiments. The animals were divided randomly into test groups (n = 5). The first group which served as control received 0.3 mL DMSO, the second group was treated with indomethacin (10 mg/kg i.p) as a positive control and the other test groups received tryptanthrin (6, 12 and 24 mg/kg i.p).

After one hour, all the animals were injected intrapleurally with carrageenan (0.1 mL) on the right side of the thorax. Two hours later, the mice were anaesthetized with chloroform, followed by the washing of the pleural cavity with distilled water.

The lungs of the animals were dissected free from the trachea and weighed. Pulmonary edema was considered to be reflected when there are significant changes in the test "wet-lung weight" in comparison to the distilled water-treated controls [40].

The following formula was used to calculate pulmonary oedema:

$$\text{Pulmonary oedema} = \frac{\text{wet lung weight}}{\text{body weight}}\ \text{X}\ 10000$$

2.4.2. Analgesic activity

Albino mice were divided into five groups of five animals each. The first group received 0.3 mL of DMSO as the negative control, the second group received acetylsalicylic acid (ASA) (100 mg/kg) which served as the positive control, while mice of third, fourth and fifth groups received 3 doses (6, 12 and 24 mg/kg) of tryptanthrin, respectively. Evaluation of the analgesic property of tryptanthrin was carried out using the chemical and thermal noxious stimuli.

2.4.2.1. Acetic acid induced writhing. Mice, randomly divided into five groups of five animals each, were treated with three graded doses (6, 12 and 24 mg/kg) of tryptanthrin via intraperitoneal administration, following the method of Siegmund and co-workers [41]. The first and second groups received DMSO (0.3 mL) and ASA (100 mg/kg), serving as the negative and positive controls, respectively. The other test groups (3^{rd}, 4^{th} and 5^{th}) received 3 doses of the test compound. One hour after treatment, the characteristic writhing response was induced in the animals in each group by administration of 0.1 mL of 3% acetic acid. The number of writhings occurring for 30 min was recorded.

Table 1. Sodium borohydride reduction of isatin (6.8 mmol) under solvent-free microwave irradiation.

Entry	Conditions	Time (min)	Products (% yield)	R_f value
1	SiO_2 (10.0 g), $NaBH_4$ (1.2 equiv)	5	NR	-
2	SiO_2 (5.0 g), $NaBH_4$ (2.3 equiv)	5	NR	-
3	SiO_2 (5.0 g), $NaBH_4$ (2.3 equiv)	10	**1** (26 %), P2, *2	0.90, 0.82, *0.48
4	SiO_2 (5.0 g), $NaBH_4$ (2.3 equiv)	20	**1** (30 %), P2, *2	0.88, 0.81, *0.45
5	Al_2O_3 (acidic) (5.0 g), $NaBH_4$ (2.3 equiv)	20	NR	-
6	Al_2O_3 (basic) (10.0 g), $NaBH_4$ (2.3 equiv)	5	NR	-
7	Al_2O_3 (basic) (10.0 g), $NaBH_4$ (2.3 equiv)	10	**1** (32 %), *2	0.87, *0.44
8	$MgSO_4.7H_2O$ (10.0 g), $NaBH_4$ (2.3 equiv)	10	NR	-
9	$MgSO_4.7H_2O$ (10.0 g), $NaBH_4$ (2.3 equiv)	30	**1** (12 %), P2, P3, *2	0.88, 0.82, 0.75, *0.45
10	$^{+}$**2**-N-$COCH_3$, Al_2O_3(basic) (10.0 g), $NaBH_4$ (2.3 equiv)	5	NR	-
11	$^{+}$**2**-N-$COCH_3$, Al_2O_3(basic) (10.0 g), $NaBH_4$ (2.3 equiv)	20	**1** (20 %), *2	0.88, *0.46

NR = No Reaction; *2 = unreacted isatin; P2, P3 = unidentified products; $^{+}$**2**-N-$COCH_3$ = 1-acetylisatin

2.4.2.2. Tail immersion test. The mice in the test groups were first treated with different doses of the compound (6, 12 and 24 mg/kg) intraperitoneally, while ASA (100 mg/kg) and 0.3 mL of DMSO were intraperitoneally administered to the control groups. One hour after compound administration, about 5 cm of the tail of each mouse was immersed into warm water bath maintained at 55 ± 1 °C and the tail withdrawal time (i.e., the reaction time) was taken as the time (in seconds) taken by animal to withdraw the tail clearly out of the water bath [42].

2.4.2.3. Hot plate test. Different doses of the test compound and standard drug were given to the test groups of mice (5 mice per group) as described above by intraperitoneal injection route. The negative control group of mice received DMSO (0.3 mL/kg i.p.) only. The control mean reaction time (in seconds) was determined and recorded. One hour following the test agent or reference drug administration, individual animal was placed on a hot plate maintained at 55 ±1 °C and the time taken by each of the mice to lick the fore paw was taken as the reaction time [43].

2.5. Statistical analysis of results

Data are expressed as the mean ± the standard error of the mean and analyzed using one way analysis of variance (ANOVA) followed by Tukey's post-hoc test, using GraphPad InStat (GPIS) software, version 3.06. For all the data obtained, the level of significance was set at $p < 0.05$.

2.6. Molecular docking studies

The 3D structure of the protein 1CX2 (cyclooxygenase 2) was downloaded from the protein databank, rcsb.org, complexed with a selective cyclooxygenase inhibitor, S58. The 3D structures of the docked compounds, celecoxib and tryptanthrin were generated with Chem3D Ultra 12.0. The protein and the studied compounds were prepared for docking using MGL tools 1.5.6. The prosthetic group, other bound small molecules and water were removed from the protein before docking. The bound inhibitor, S58 was re-docked with the protein, using the grid dimensions in Amstrong units, size (x,y,z) = (40, 40, 40) and center (x,y,z) = (28.684, 28.603, 9.285) with AutoDock Vina 1.1.2 from the molecular graphics lab [44] and setting the following residues in the protein as flexible, HIS90, ARG120, GLN192, VAL349, LEU352, SER353, TYR355, TYR385, TRP387, ARG513, ALA516, PHE518, VAL523, GLY526, ALA527, LEU351. The docking calculation was complete in one hour on a macintosh machine, mac OS Sierra, with an intel core i5, 2.5 GHz processor. The rmsd of the docked S58 in comparison with the native S58 was estimated as 1.30 Å with a binding energy of -11.2 kcal/mol. The binding energy of the other docked compounds, which were complete in approximately one hour as well, and their interactions are summarized in

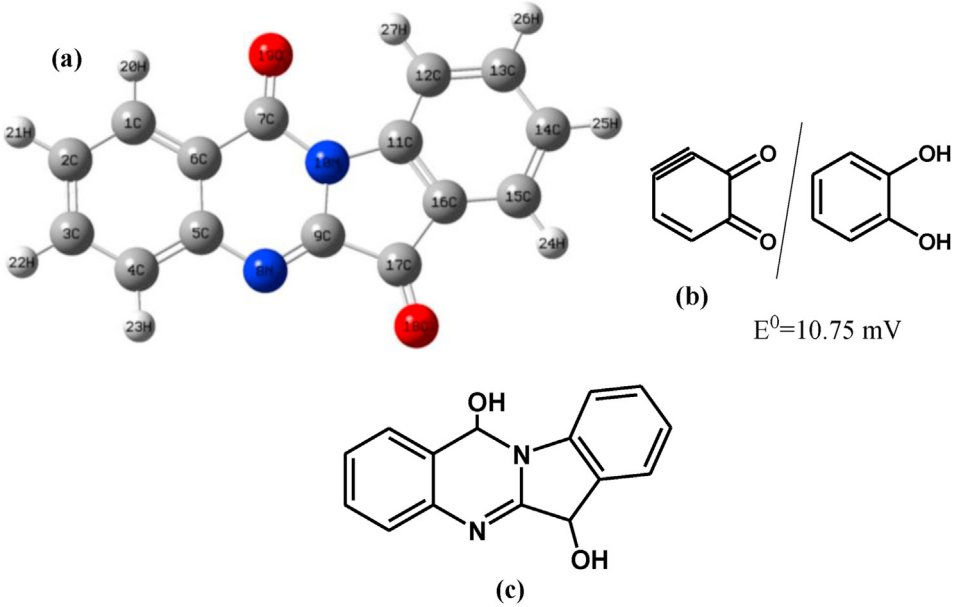

Figure 1. (a) Optimized structure of tryptanthrin (I_{oxi}) (b) Four-electron oxidized/reduced forms of catechol (**II**) (c)Reduced form of tryptanthrin (I_{red})

Table 4. The docking results and 3D structure of the protein were visualized using Pymol (v 1.7.4.5). Pymol was also used to determine the interactions of the compounds with the protein and estimate bond distances as well snapshots of the compounds docked within the binding site of the protein.

2.7. Computational details

Geometry optimization of the initial guess structure to a minimum was carried out without symmetry constraints at the B3LYP/6–311++G (2df, 2pd) level, using Gaussian 03W [45, 46]. The choice of method was informed by the previous benchmarking done by our group [47] for molecules containing similar atoms and bonds as Tryptanthrin (Figure 1a). Our observation from the benchmarking is that the geometrical and electronic properties, which form part of our primary interests in the current study, were most sufficiently predicted by the adopted method. Another reason for our choice of this method is the fact that the accuracy of the thermodynamic parameters that is needed to predict the anti-oxidant property is a function of the geometric data, and which was satisfactorily done by the method adopted. Single point frequency and time-dependent self-consistent field (td-scf) calculations were performed at the same level of theory used for the optimization. The vibrational analysis report shows no negative frequency, indicating that the resulting optimized structure is a minimum on the potential energy surface (PES). The TD-SCF calculation was done for $N = 20$ states. ^{1}H and ^{13}C NMR were obtained by Gauge Independent Atomic Orbital (GIAO) method [48] at the B3LYP/6-31G level of theory. Scaling factors for both NMR and IR calculations is 1.000.

2.7.1. Gas- and solution-phase free energy calculations

Isodesmic reaction scheme was employed in the calculation of the four-electron redox potential of the studied compound (Scheme 2). The molecule of reference (catechol) with its four-electron redox potential value is presented in Figure 1b, while the reduced form of tryptanthrin is shown in Figure 1c. Integral equation formalism polarizable continuum model (IEF-PCM) [49, 50] was adopted for the solvent-phase computation using water as solvent. The standard reduction potential of **I** had been calculated using a modified literature procedure [51, 52].

Conversion of total electronic energies (E_{el}) to Gibbs energies (G^o) was achieved using the zero-point energy (ZPE), thermal correction (TC) and entropy (S) at 298.15 K according to Eq. (1):

$$G_s^o = (E_{el_s} + ZPE_s + TC_s) - TS_s \quad (1)$$

The subscript *s* in Eq. (1) denotes the species whose property is being computed.

Using the thermodynamic cycle outlined in Scheme 3, the change in free energies of the gas and solution phase reactions are defined according to Eqs. (2) and (3) [51, 52]:

$$\Delta G_{gas}^o = G_{gas}^o(\mathrm{I_{red}}) + G_{gas}^o(\mathrm{II_{oxi}}) - G_{gas}^o(\mathrm{I_{oxi}}) - G_{gas}^o(\mathrm{II_{red}}) \quad (2)$$

$$\Delta G_{sol}^o = \Delta G_{sol}^o(\mathrm{I_{red}}) + \Delta G_{sol}^o(\mathrm{II_{oxi}}) - \Delta G_{sol}^o(\mathrm{I_{oxi}}) - \Delta G_{sol}^o(\mathrm{II_{red}}) \quad (3)$$

where ΔG_{gas}^o is the standard Gibbs energy of the reaction in the gas phase and ΔG_{sol}^o is the net solvation energy of the reaction in solution phase (Table 7). The overall change in Gibbs energy (ΔG_T^o) for this system is given by Eq. (4) [51, 52]:

$$\Delta G_T^o = \Delta G_{gas}^o + \Delta G_{sol}^o \quad (4)$$

The redox potential of **I** can be obtained according to Eq. (5) [51, 52, 53]:

$$\Delta G_T^o = -nF\left(E_{I_{oxi/red}}^O - E_{II_{oxi/red}}^O\right) \quad (5)$$

where *n* is the number of electrons transferred ($n = 4$ in this case), *F* is the Faraday constant and E_{II}^ooxi/red is the four-electron redox potential value for cyclohex-3-en-5-yne-1,2-dione/catechol (reference molecule) which was extrapolated from the experimental one-electron redox potential of catechol [54].

Ascorbic acid (AA) was subjected to the same treatments described in Scheme 3 following the four-electron isodesmic reaction, Scheme 4, to obtain its ΔG_T^o and four-electron reduction potential ($E_{AA_{oxi/red}}^o$) value.

3. Results and discussion

3.1. Chemistry

The original intention of the present research work was to synthesize 2,3-dihydroindole-2,3-diol **10a** via reduction of isatin **2,** using sodium borohydride on solid support under microwave irradiation, in a manner similar to reduction of ketones [55, 56].

Isatin **2** and its 1-acetyl derivative **2'** were reduced by sodium borohydride supported on solid matrices (SiO_2, Al_2O_3, $MgSO_4$) with the assistance of microwave irradiation for different reaction times. Treatment of isatin **2** (6.8 mmol) with $NaBH_4$ (7.9 or 15.9 mmol) on silica under high microwave (mw) irradiation for five minutes produced no products (Table 1, entries 1 and 2). A longer reaction time had beneficial effect. MW irradiation of **2** (6.8 mmol) with $NaBH_4$ (15.9 mmol) on silica for 10 min gave two products plus unreacted **2,** with the less polar product ($R_f = 0.89$) identified as tryptanthrin **1**in low yield (26 %) and the more polar product, P2 ($R_f = 0.82$), unidentified. The unreacted starting material, isatin, has an R_f value of 0.48 (toluene:ethyl acetate, 5:2, v/v) (Table 1, entry 3). Irradiation for 20 min still afforded the two products plus unreacted isatin with only a slight increase in percentage yield of **1** (30 %) (Table 1, entry 4). Additionally, the reduction of isatin **2** was investigated with $NaBH_4/Al_2O_3$ (acidic): Irradiation of isatin (6.8 mmol) with $NaBH_4$ (15.9 mmol) on alumina (acidic) for 20 min gave no reduction product (Table 1, entry 5). The use of alumina (basic) instead of alumina (acidic) gave a different result. As was observed for reaction on silica gel, there was no reaction after irradiation for 5 min on basic alumina solid support (Table 1, entry 6). However, irradiation of the reactants for 10 min afforded only tryptanthrin **1** in 32 % yield, with some unreacted isatin (Table 1, entry 7). Change of solid support to hydrated magnesium sulfate produced no reaction after mw irradiation for 10 min (Table 1, entry 8). However, irradiation for 30 min resulted in three products: compound **1,** two unidentified compounds and unreacted

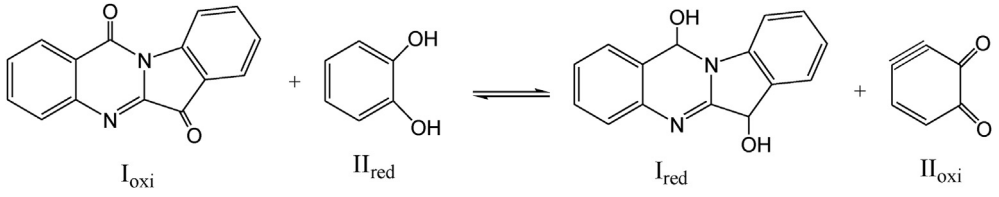

I_{oxi} II_{red} I_{red} II_{oxi}

Scheme 2. Isodesmic redox-conversion of compound (**I**) by catechol (**II**).

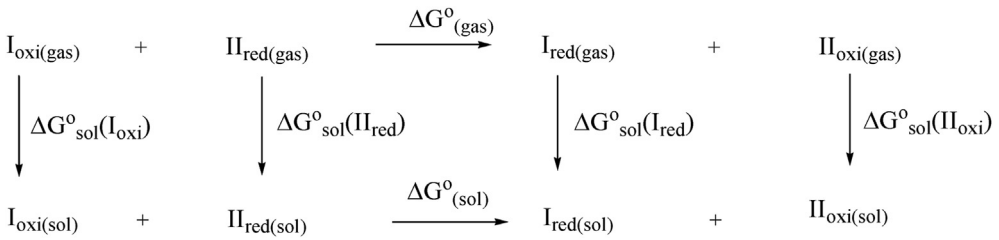

Scheme 3. Thermodynamic cycle employed to obtain compound **I** redox potential.

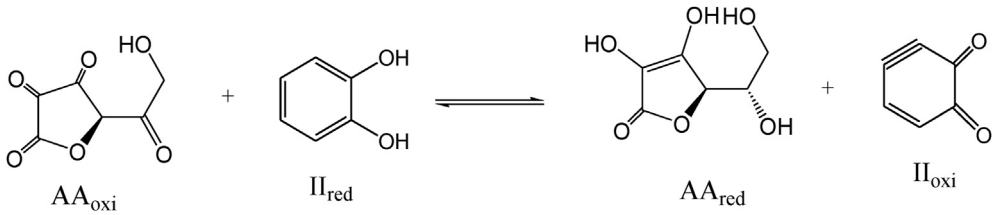

Scheme 4. Isodesmic redox-conversion of ascorbic acid (AA) by catechol (**II**).

starting material **2** (as monitored by thin layer chromatography (tlc)) (Table 1, entry 9).

Sodium borohydride reduction of isatin derivatives have been examined previously under different reaction conditions [57, 58] (Scheme 5). In the reported reactions, 5-nitroisatin **2′a** upon reaction with $NaBH_4$ in methanol, at 1–5 °C, gave a ring-opened product, methyl 2-amino-5-nitrophenylglyoxylate **8** in about 30 % yield, with the methanol acting as the attacking nucleophile at the N–C=O bond of **2'.** On the other hand, $NaBH_4$ reduction of **2′**with an electron-withdrawing group at position 1 (e.g., 1-acetylisatin, **2′b**), at room temperature in the presence of alcohol, easily afforded a further reduced, ring-opened product, ethyl 2-acetamidomandelate **9,** while reduction in the presence of a non-nucleophilic solvent, like tetrahydrofuran, gave the unopened indole ring product, 1-acetyl-2,3-dihydroindole-2,3-diol **10b** in about 30% yield [58].

It has been established that electron-withdrawing groups on nitrogen atom of isatin and its derivatives make them to easily undergo nucleophilic, ring-opening reactions at the N1–C2 bond to give phenylglyoxylic acid derivatives [59, 60]. Hence 1-acetylisatin **2′b** was subjected to reduction reaction with sodium borohydride supported on solid basic alumina matrix to see the effect of the electron-withdrawing group. The results showed that the reduction of 1-acetylisatin (5 mmol) with 2 M equivalent of $NaBH_4$ in the presence of basic Al_2O_3 behaved like unsubstituted isatin **2.** Irradiation for 5 min gave no reaction (Table 1, entry 10). Prolonged irradiation for 20 min afforded tryptanthrin **1** in 20% yield together with de-acetylated, unreacted isatin (Table 1, entry 11).

The reductive synthesis of **1** can be rationalized through a first ring-opening step via reaction with water, to give an intermediate 2-aminoglyoxylic acid, which reacts with another molecule of isatin via concomitant loss of CO_2 and acylation at position 1 to give 1-(2-aminobenzoyl)isatin, which condenses further intramolecularly with the lactam carbonyl group, allowing tryptanthrin **1** to be obtained (Scheme 6).

3.2. *Effect of tryptanthrin on carrageenan-induced edema in mice*

Carrageenan-induced mouse paw edema as an assay was used to estimate the effects of synthetic tryptanthrin on acute inflammation and pulmonary oedema induced inflammatory responses and the effects are

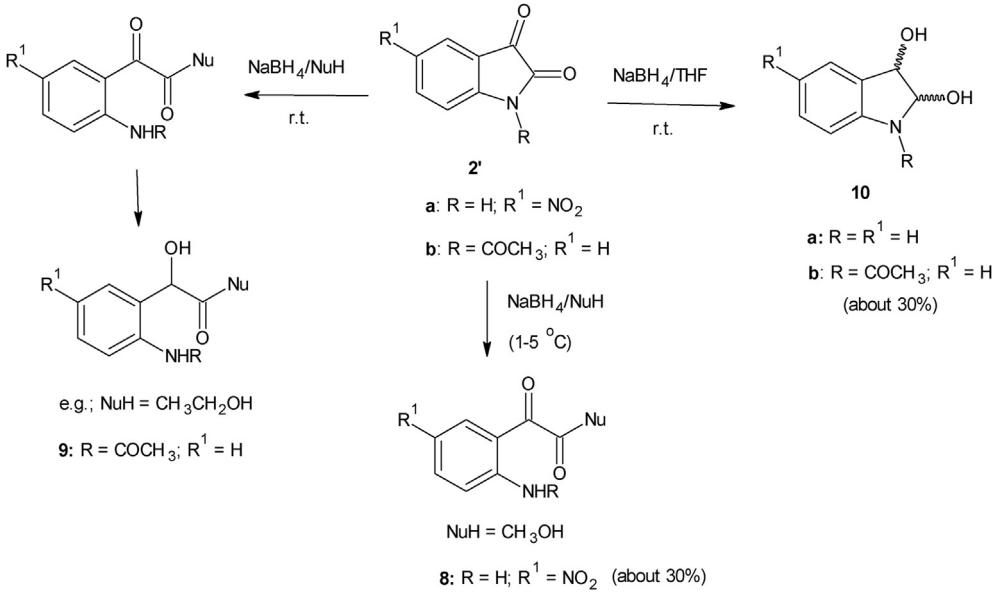

Scheme 5. Sodium borohydride reduction of some substituted indole-2,3-dione (isatin) [57, 58].

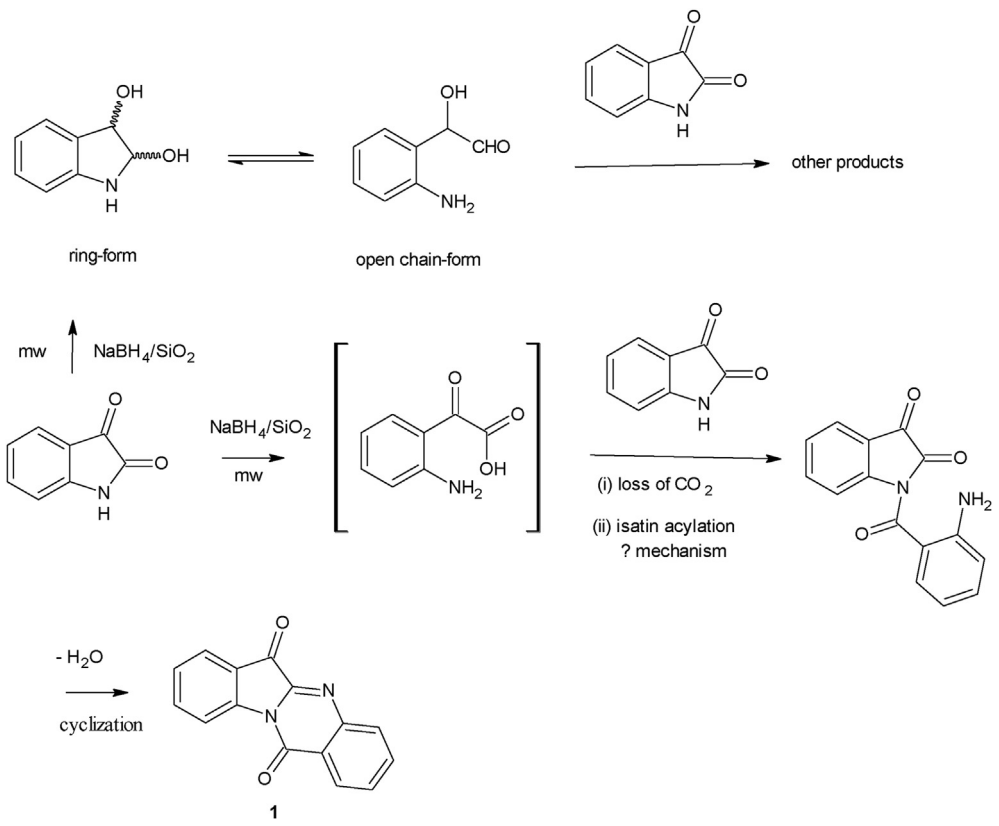

Scheme 6. Possible rationalization of sodium borohydride reduction of isatin to tryptanthrin

presented in Table 2, while the compound's effects on pains induced by chemical (acetic acid) and thermal stimuli are reported in Table 3.

The results showed that tryptanthrin dose-dependently inhibits oedema and pain formation in all the models used. The agent also exhibited significant higher effects in its anti-inflammatory and analgesic activities better than positive drugs (aspirin and indomethacin) being currently used in the treatment and management of acute and chronic forms of pain and inflammatory disorders.

Inflammation is the body's protective response (or a defense mechanism), consisting of a series of processes, that is generated physiologically by the body to guard the body against infection, injury or irritation and hasten-up the recovery process. Signs and symptoms of inflammation include: pain, redness and swelling, temperature and loss of functions [61]. However, inflammation that is unchecked leads to chronic inflammatory disorders and pain which can manifest both peripherally and centrally. The initiation and maintenance of inflammation in injured cells is by the overproduction of cytokines, nitric oxide, prostaglandins and leukotrienes, which are produced by separate enzymatic pathways, viz the cyclo-oxygenase (COX) and lipoxygenase (LOX) pathways [62]. The cyclooxygenase and lipoxygenase pathways are used for potential interventions against inflammation because some of the anti-inflammatory drugs have been observed to inhibit the lipoxygenase pathway and some

Table 2. The effects of synthetic tryptanthrin agent on acute inflammation and pulmonary oedema induced inflammatory responses in mice.

Compound	Doses (mg/kg)	Acute Inflammation	% Inhibition (AI)	Pulmonary Oedema	% inhibition (PO)
Negative control (DMSO)	0.3 mL	0.109 ± 0.006	0	83.3 ± 2.2	0
Tryptanthrin	6	0.048 ± 0.011*	55.963	61.98 ± 10.78	25.59
	12	0.036 ± 0.022*	66.972	56.38 ± 9.32	32.31
	24	0.022 ± 0.007*	79.816	54.77 ± 11.59*	34.25
Indomethacin	10	0.038 ± 0.005*	65.137	60.0 ± 1.1	27.97

Values represent means ± SEM of 5 animals *p < 0.05.

Table 3. The effects of synthetic tryptanthrin agent on tail immersion, hot plate (as thermal stimuli), and acetic acid induced writhing (as chemical stimulus) induced pain responses in mice.

Compounds	Doses (mg/kg)	Tail immersion (sec)	Hot plate reaction (sec)	Acetic acid induced writhing
Negative control (DMSO)	0.3 mL	1.7 ± 0.30	8.9 ± 0.57	51.0 ± 6.08
Tryptanthrin	6	2.69 ± 0.78	11.38 ± 2.67*	75.40 ± 9.85
	12	2.08 ± 0.33	14.96 ± 2.64*	60.80 ± 8.19
	24	2.46 ± 0.64	17.50 ± 2.68**	20.60 ± 3.49**
Acetysalicyclic acid	100	4.5 ± 0.30*	16.2 ± 2.90**	19.6 ± 0.80**

Values represent means ± SEM of 5 animals *p < 0.05, **p,0.01.

Table 4. Residues within 4 Å of the native S58 and comparison with interacting residues of the docked S58, celecoxib and tryptanthrin.

Compounds	Residues within 4 Å of the docked compounds/bound inhibitor	Binding energy (-kcal/mol)	Polar contacts
1CX2 with bound inhibitor (S58)*	**HIS90**, **ARG120**, **GLN192**, **VAL349**, **LEU352**, **SER353**, **TYR355**, **TYR385**, **TRP387**, **ARG513**, **ALA516**, **PHE518**, **VAL523**, **GLY526**, **ALA527**, **LEU351**		
S58	**GLN192**, **VAL349**, **LEU352**, **SER353**, *GLY 354*, **TYR355**, *LEU359*, **TYR 385**, **TRP387**, **ARG513**, **ALA516**, *ILE517*, **PHE518**, **VAL523**, **GLY526**, **ALA527**, **LEU531**	11.2	HIS90 (flex, 2.7A); ARG513 (flex, 2.6 & 2.2A); SER353 (2.1A)
Celecoxib	**HIS90**, **VAL349**, **LEU352**, **SER353**, **TYR355**, **TYR385**, **TRP387**, **ARG513**, **ALA516**, *ILE517*, **PHE518**, **VAL523**, **GLY526**, **ALA527**, **LEU531**	11.3	HIS90 (flex, 2.6A); TYR355 (flex, 2.9A)
Tryptanthrin	*ALA199*, *PHE200*, *GLN203*, *VAL295*, **TRP387**, *HIS388*, *LEU390*, *LEU391*, *LEU408*, *HEME*	9.7	

* The residues in bold font are those associating with the native S58 in the designated binding site that are also associating with the other compounds docked with the protein. The residues in italics are those aside from the ones interacting with the native ligand that are also interacting with the docked compounds. Almost all italicized residues for tryptanthrin indicate that the tryptanthrin must have bound to a different site in the protein.

inhibit cyclooxygenase pathway [63, 64]. The lipoxygenase pathway and its increased activity has a role to play in the pathophysiology and aggravate asthmatic symptoms.

It has been shown scientifically that tryptathrin is a potent inhibitor of prostaglandin and leukotriene synthesis in various inflammatory cell lines. It has also been shown to be a selective inhibitor of cyclooxygenase 2 (COX-2), inducible nitric oxide synsthase (iNOS; NOS II) expression and other cytokines like IFN-γ and IL-2. It inhibits P-glycoprotein (Pgp) (expressed by the MDR1 gene) and reverses doxorubicin resistance on breast cancer cells [15, 26, 65, 66].

The anti-inflammatory activity of a test compound can be evaluated on manifestations accompanying the inflammatory reaction such as oedema, leukocyte influx to inflamed tissue and increase in vascular permeability. In this study, tryptanthrin reduced carrageenan-induced mice paw oedema in a dose-dependent manner compared to control group and a significant difference was observed between the inhibition at 12 mg/kg of tryptanthrin and indomethacin (10 mg/kg). The injection of carrageenan in the mouse paw has been reported to produce a two-phased response [67]. The first phase, observed during the first hour, is mediated by the release of histamine and serotonin [68], followed by the second accelerating phase of swelling caused by the release of prostaglandin, leukotrienes, bradykinin and lysozyme. In addition, the second phase of oedema has been reported to be sensitive to both clinically useful steroidal and non-steroidal anti-inflammatory agents [69]. Even though Ruster's research group [70] reported an inhibitory activity of indolin-2-one (an indole derivative) from *Isatis* species on compound 48/80-induced histamine release from mast cells, tryptanthrin (a quinazoline ring fused to an indole moiety) from the same plant did not inhibit histamine release, which could indicate that tryptanthrin is not acting on first phase of inflammation. However, pre-treated with tryptanthrin resulted in a significant oedema inhibitory response 2 h following carrageenan injections, thus suggesting that tryptanthrin may act by suppressing the later stage of the inflammatory process via the inhibition of cyclooxygenase, the rate-limiting enzyme involved in the biosynthesis of prostaglandins.

The effect of tryptanthrin on pulmonary oedema in this study corroborate the work of Feng's group on anti-inflammatory effect of SQC-β-CD on lipopolysaccharide-induced acute lung injury [71]. Lipopolysaccharide-induced inflammatory reaction has been linked with the production of LOX [72], and tryptanthrin inhibited the production of LOX in their study. Also, tryptanthrin has been found to suppress the activation of the LPS-Treated BV2 Microglial Cell Line [73]. Yang and co-workers [28] demonstrated the potency of tryptanthrin derivatives as potent inhibitors of Indoleamine 2,3-Dioxygenase with therapeutic activity on Lewis Lung Cancer (LLC) Tumor-Bearing Mice. Cancer cells have been shown to emerge in form of an inflammatory response, therefore in this study, tryptanthrin has been shown to lend credence to possible way in which inflammatory response in the lung cell could be curtailed.

3.3. Analgesic activity

Pain is a signal or an indication that the tissue is damaged. It is a clear indication and sign of inflammation. Since chronic inflammation can be observed both at the peripheral and central, the analgesic effect on tryptanthrin was evaluated of peripheral pain model in acetic acid induced writhing and centrally mediated pain as shown in both hot plate reactions and tail immersion in hot water. The results are shown in Table 3. In all these models, it is shown that the cyclo-oxygenase (COX) and lipoxygenase (LOX) pathways are involved. Hence the effects of tryptanthrin on these models are indication of analgesic activity. To complement our study, tryptanthrin (an alkaloid) found in the *Indigo naturalis* plant has been found to block the itching, tightness and pain associated with chronic, inflammatory skin conditions such as eczema and psoriasis. According to research studies, tryptanthrin blocks the itching, produced tightness. Tryptanthrin molecule which was incorporated into medications as lotions, ointment is a potent anti-inflammatory compound that inhibits prostaglandins, in other words, it blocks pain. It also helps soothe irritated skin and blocks leukotrienes, which are components of inflammation.

There are also indications that tryptanthrin could be blocking nerve cells directly as a means to provide eczema itch relief [74, 75].

3.4. Molecular docking studies

The inhibitory potential of the synthesized compound, tryptanthrin, was investigated by molecular docking using the software, autodock vina. The binding energy of the compound with the protein (cyclooxygenase 2) was estimated, its binding pose and interactions with amino acid residues within the binding site of the protein were also determined.

The binding energy of the docked compounds and their interactions are summarized in Table 4.

The residues set as flexible in the protein are among the residues within 4 Å of the native ligand (S58) which may also be described as residues within the binding site of the protein for S58. Upon redocking, it is observed that the S58 is docked (with binding energy of -11.2 kcal/mol) in the same site that the residues have been set as flexible (Figure 2b). Celecoxib also having similar structure with S58 (with a Br replaced by a CH_3 group) also docked into the same site that S58 docked into, with binding energy -11.3 kcal/mol. Tryptanthrin, however, preferred to dock into the cavity in the protein that seats the prosthetic heme group (Figure 2c & d), having a lower binding energy (-9.7 kcal/mol). Visualizing the docking results with pymol (version 1.7.4.5), it is clear that the tryptanthrin prefers the pocket housing the heme group

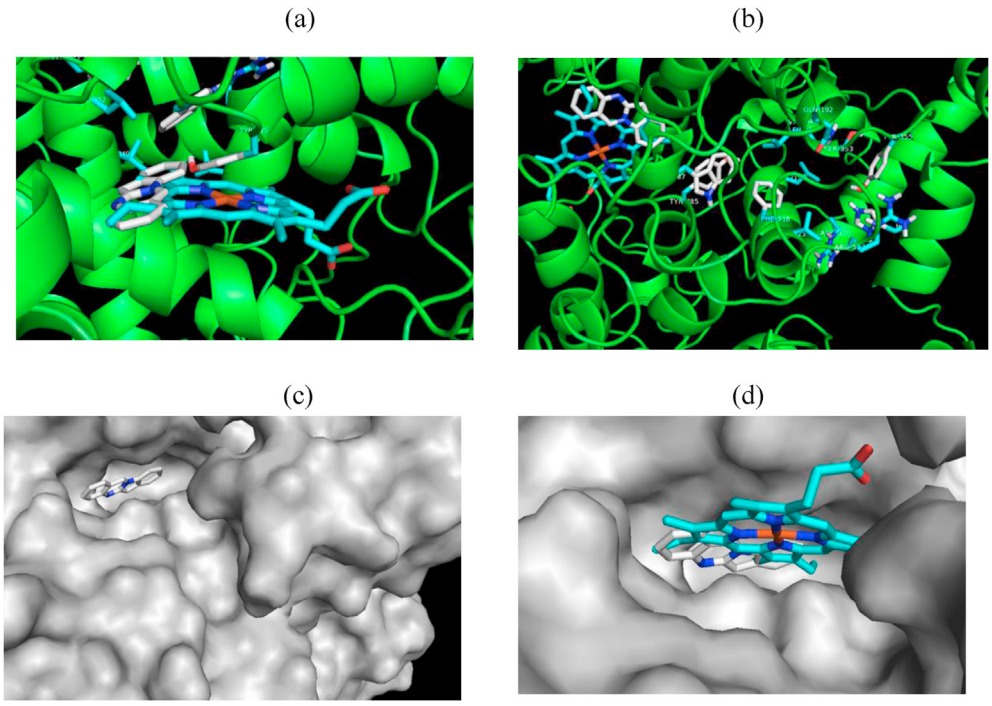

Figure 2. (a) Cartoon rendering of the protein showing tryptanthrin overlapping with heme in the same site. (b) Cartoon rendering of the protein showing the flexible residues at the S58 binding site adjacent to the site where heme occupies in the protein. (c) A surface rendering of the protein showing tryptanthrin lodged in the pocket that seats the heme (without the heme). (d) Another surface rendering showing the tryptanthrin overlapped with the heme in the heme pocket.

which implies that there might be some form of interactions with the heme preventing the heme from functioning appropriately in its catalytic role within the protein (Figure 2a & d).

The result obtained for the selective inhibitors (S58 and celecoxib) is consistent with existing knowledge of their interactions with the COX-2 isozyme [76, 77, 78]. The selective inhibition of these compounds is based on the fact that the drugs can bind to parts of the COX-2 isozyme that are not available in the COX-1 isozyme. The sulfonamide moiety of the drugs fit into a hydrophobic side pocket and forms hydrogen bonds with ARG513, HIS90 and the peptide bond of PHE518; interacts closely with TYR355, TYR385, VAL523 in the adjacent side of the hydrophobic pocket close to the heme pocket. All the residues mentioned above are among those within 4 Å of the re-docked S58 with hydrogen bonds between the sulfonamide and ARG513 and HIS90. The tryptanthrin docked with COX2 under the same conditions as the S58 and celecoxib having affinity for the heme pocket implies that it might not inhibit the isoforms selectively and its therapeutic effect as an analgesic/anti-inflammatory agent might be moderate.

3.5. Computational studies

The optimized structure of tryptanthrin which would later be referred to in this paper as the oxidized form of tryptanthrin ($\mathbf{I_{oxi}}$) is presented in Figure 1a. Tryptanthrin and its derivatives are known to exhibit a number of biological activities as highlighted in section 1. The mechanism(s) of action of the pharmacological effects at the molecular level had been reported [65, 79]. However, the mechanism of the free-radical scavenging activity has not been theoretically investigated. It is known that antioxidants and free radical scavengers can exert an anti-inflammatory effect [80].

In this work, the free-radical scavenging ability has been estimated by comparing the thermodynamic four-electron redox potentials of tryptanthrin and ascorbic acid using catechol as the reference molecule. The same methods of calculations were employed for all the studied molecules. It is worthy of note that the spectroscopic characterizations of tryptanthrin and its derivatives have been extensively reported [12, 23, 81, 82], therefore, the spectroscopic information presented here had been used only to validate the optimization method employed in this study.

The bond lengths and bond angles of the skeletal structure have been compared with the crystallographic data [81] in Tables S1 and S2 of the supporting document. We found the low mean percentage errors (% MPE) obtained to indicate high level of agreement between the calculated and the experimental structures. The calculated NMR, IR and UV-visible data were based on this structure in Figure 1a. The ^{13}C (Table S3 in the supporting document) and ^{1}H NMR (Table 5) data have been presented along with those obtained from experiments (in our laboratory). For the ^{13}C NMR (Table S3), the reference shielding δ values were determined by HF/631G method as 199.10 ppm using methane (CH_4), and as 199.99 ppm using tetramethylsilane (TMS). Both internal reference standards (CH_4 and TMS) displayed good reproducibility of the experimental data with respect to their low % MPE values (Table S3). The TMS however, showed a better agreement with the experiment, judging from its lower %MPE. The ^{1}H NMR data determined with TMS as

Table 5. Experimental and calculated ^{1}H NMR data.

*Experiment ppm	Calculated **(TMS) ppm	% Error
7.41 [1H, *d*]	6.97	5.94
7.66 [1H, *dt*]	7.29	4.83
7.77 [1H, *dt*]	7.31	5.92
7.84 [1H, *dt*]	7.42	5.36
7.91 [1H, *d*]	7.55	4.55
8.00 [1H, *d*]	7.61	4.88
8.42 [1H, *dd*]	8.32	1.19
8.60 [1H, *d*]	8.49	1.27
Mean percentage error (% MPE)		4.08

* (Our lab.)

** Reference shielding δ value calculated by HF/6-31G, TMS = 32.60 ppm, information in square brackets = proton quantity and multiplicities.

Table 6. Wavenumbers (experiment and theory) and band assignments for compound I_{oxi}.

Experimental[a]	Calculated	Band assignments[b]
1727	1796	υC = O (ketone)
1685	1736	υC = O (amide)
1594	1631	υC = C
1314	1323	
1113 (w)	1120	
1040 (w)	1029	
755	777	γC-H (Ar)

[a] Experimental data as obtained from our laboratory.
[b] υ: stretching; γ: out-of-plane bending.

reference are also in good agreement with the experiment (Table 5). Similarly, our calculated and experimental IR data (Fig. S1 and Table 6) were found to correlate satisfactorily (Fig. S2).

It is reasonable to think of a correlation between free-radical scavenging ability and electronic property of molecules [83]. While the relationship between free-radical scavenging ability and electronic properties of some coumarin derivatives had been reported by Al-Majedy and *co.* [83], this study compared two properties which were obtained by computation, reduction potentials (E^{θ}) and electronic properties, to establish the link between them. It would also provide a basis for more logical interpretation of molecular electronic parameters with respect to redox processes than has heretofore been done. Electronic properties, such as HOMO (highest occupied molecular orbital), LUMO (lowest unoccupied molecular orbital), dipole moment (μ), HOMO-LUMO gap, ionization potential (IP) and electron affinity (EA), of tryptanthrin were computed and compared with literature values for ascorbic acid [83]. In addition, the computed electronic parameters for tryptanthrin and literature values for ascorbic acid [83] were compared with the calculated E^{θ} for the two compounds. We have also included the computed E^{θ} literature value of ascorbic acid [84] for analogy. Interestingly, there appears to be no detailed theoretical study on the electronic and antioxidant properties of tryptanthrin hitherto. One finds this surprising owing to the clout of tryptanthrin in the medical fields [12, 17, 23, 24, 65, 79, 81, 82, 85]. With this in mind, the results of the TD-DFT calculation carried out on the tryptanthrin molecule (Figure 3) have been included to provide theoretical insight into the molecule's absorption properties.

Two absorption spectral bands at 236 and 373 nm are evident in the calculated absorption spectrum (Figure 3). It is typical to find a relatively high energy band around 200 nm for a benzene moiety [86, 87]. The absorption at 236 nm (λ_{236}) results mainly from the transition of electrons from [HOMO-3] → [LUMO+1] (56.37%), [HOMO] → [LUMO+2] (30.06%) and [HOMO-7] → [LUMO] (13.57%). The percentage contributions of the orbital transition to the absorption at the specific wavelength are quoted in the parentheses. The band described by the above-mentioned transitions is red-shifted as expected for a di-benzene molecule, relative to the absorption band of pure mono-benzene at 203.5 nm [86]. It is noteworthy that the solvation effect that could also be responsible for the red-shift has been excluded in our calculation [87]. The absorption at 373 nm results from [HOMO] → [LUMO] (100%) and corresponds to the π → π* transition.

For the absorption at 236 nm, [HOMO-3] → [LUMO+1] and [HOMO] → [LUMO+2] transitions contributed most significantly. The calculated energy levels and the molecular orbitals presented in Figures 4 and 5 respectively may be used to explain some of these molecular orbital (MO) transitions. The electron density distributions on the molecular orbitals in Figure 4 have been classified using lines. The lines have been coded according to their positions and orientations. For example, the direction and orientation of the electrons in the [HOMO-3] is similar to that of [LUMO+1] (as indicated by the lines), hence the transition between these orbitals (i.e. $A_{-31} \rightarrow A_{-31}$). This to a reasonable approximation shows that their symmetry structures are closely similar. It should be noted that electron densities with similar structures undergo mixing with one another, and such is accompanied by absorption/emission of radiation of appropriate wavelength. The electron density coded as B_{002} in HOMO (the red line on green and brown coefficients only) have similar structure with a part in [LUMO+2], thus explaining why these two MOs overlapped. The HOMO→LUMO transition occurred because the A_{000} structure in HOMO (red line on green coefficient only) also corresponds to the A_{000} in LUMO (longest red line only). The HOMO-LUMO gap of +0.134 a.u (~+352 kJ mol^{-1} or ~3.65 eV) obtained is within the range of the values reported for coumarins by Al-Majedy et al. [83]. Although the calculations by Al-Majedy and co-workers employed a lower 3-21G basis set, their results are still very relevant to this work as it could provide hints about the trend of the investigated parameters. The values of the parameters could provide all the information needed in potential anti-oxidants. A good antioxidant should possess a low oxidation power (high reduction potential) [88], hence must be a good electron donor. The lower band gap (HOMO-LUMO) of **1'** ($\mathbf{I_{oxi}}$) revealed its electron donor superiority over ascorbic acid (Table 7), a property that is required in a good anti-oxidant. Dipole moment values of the compound and ascorbic acid shows that the polarity of the compound is smaller compared to that of the ascorbic acid, and would therefore be less soluble in polar solvents. The IP given by $-E_{HOMO}$ indicates that the initial energy required to release an electron from a molecule in the gas phase is higher in ascorbic acid [89], Table 7. Low IP is important in the design of a good antioxidant. The IP and the HOMO-LUMO gap of the investigated molecules show good correlation as expected. The EA is given by $-E_{LUMO}$,

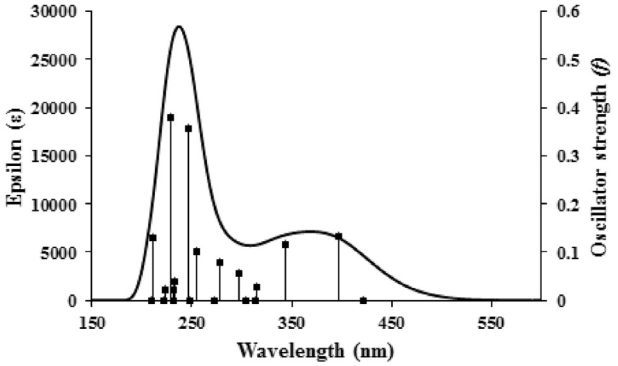

Figure 3. Calculated electronic absorption spectrum of tryptanthrin

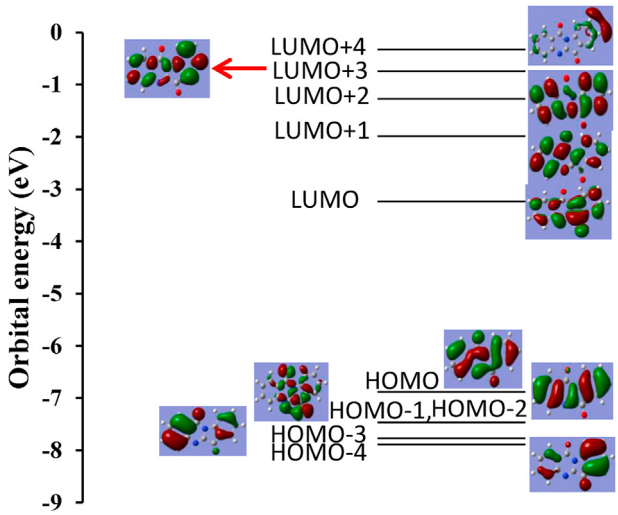

Figure 4. Molecular orbital energy levels of tryptanthrin

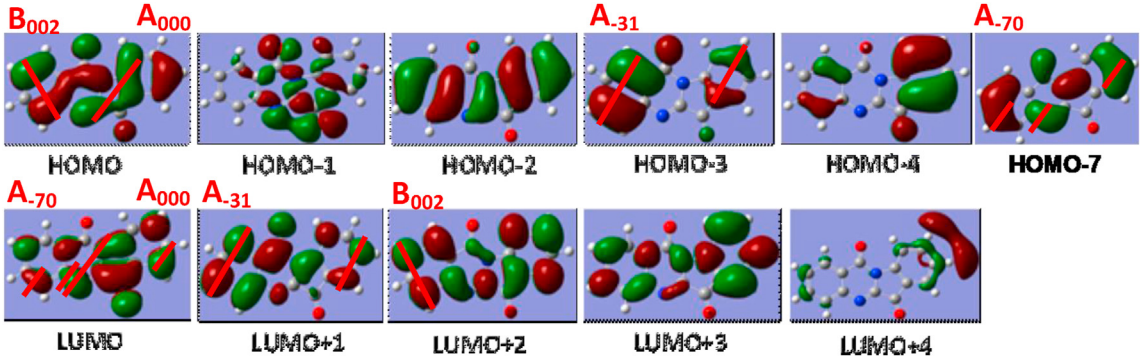

Figure 5. Molecular orbital symmetries corresponding to the different molecular energy levels of tryptanthrin

Table 7. Calculated total free energy (ΔG_T), redox potential ($E^{+}_{M/M}$) and electronic parameters of the studied compounds.

	ΔG_T (kJ/mol)	$E^{oxired}_{M/M}$ (mV)	IP (*kJ/mol*)	EA (*kJ/mol*)	*α* (*Debye*)	*HOMO* (kJ/mol)	*LUMO* (kJ/mol)	*HOMO-LUMO* (kJ/mol)
1' (I_{oxi})	478.50	-1229.0	665.21	312.73	2.1074	-665.21	-312.73	352.47
Ascorbic Acid	284.90	-727.40 (-0.281)[a]	1041.1[b]	107.77[b]	9.5490[b]	-1041.1[b]	-107.77[b]	933.19[b]

[a] Ref. [84].
[b] Ref. [83].

and is defined as the amount of energy released when an electron is absorbed by a molecule. EA is higher for ascorbic acid than for tryptanthrin, therefore the ascorbic acid would give out a higher energy than the tryptanthrin when an electron is absorbed.

The thermodynamic results for the two species supports the observations from the electronic data. The overall free-energy for the electron transfer process involving either molecule is positive (Table 7), although the ascorbic acid ΔG_Tvalue is *ca* half that of **1'**. The negative redox potential ($E^{oxired}_{M/M}$) value obtained for tryptanthrin and ascorbic acid is comparable to what was found previously by fitting experimental data to some electrode equations [84]. This agreement indicates the suitability of the procedure adopted in this work. The higher $E^{oxired}_{M/M}$ value obtained for ascorbic acid relative to tryptanthrin implies that ascorbic acid is a more electron acceptor than the tryptanthrin which is a more electron donor. Hence, tryptanthrin potentially possesses a higher antioxidant power than ascorbic acid.

Given the above, tryptanthrin shows much more effective antioxidant activity compared to ascorbic acid, however, in terms of solubility, ascorbic acid is more superior. Hence, there is need for structural modification of tryptanthrin to enhance its solubility property in order to exploit its full potential as an antioxidant. Tryptanthrin is found to possess more advantages over ascorbic acid in properties like IP, HOMO-LUMO gap and $E^{oxired}_{M/M}$.

4. Conclusion

A new method for the synthesis of the natural alkaloidal compound tryptanthrin is reported. It was carried out by reduction of isatin with solid-state-supported sodium borohydride under microwave irradiation. The compound was characterized based on elemental analysis, FT-IR, ^{1}H NMR, ^{13}C NMR and mass spectral data.

Valuable data on acute *in vivo* anti-inflammatory and analgesic effects of tryptanthrin are provided. The synthesized compound suppressed carrageenan induced inflammation and reduced pain induced chemically and thermally significantly. Analgesic and anti-inflammatory effects of tryptanthrin exert their effects through a variety of mechanisms.

The binding affinity and pose of the trypthantrin obtained from the docking study shows that the trypthantrin might have a different mechanism of action from the known clinical agents being used to manage pain and inflammation. The results also suggest that the trypthantrin may have moderate analgesic or anti-inflammatory activity based on the strength of its binding interactions and binding energy relative to the coxibs used as reference in the docking study.

The DFT methods employed have shown that compared to ascorbic acid, tryptanthrin shows higher antioxidant activity which may be improved upon by functionalizing the aromatic core to enhance its solubility in polar solvents. The calculated electronic and thermodynamic properties obtained for tryptanthrin compete well with the standard ascorbic acid.

Declarations

Author contribution statement

C.A. Obafemi: Conceived and designed the experiments; Performed the experiments; Contributed reagents, materials, analysis tools or data; Wrote the paper.

E.O. Iwalewa: Conceived and designed the experiments; Analyzed and interpreted the data; Wrote the paper.

O.A. Fadare: Performed the experiments; Analyzed and interpreted the data; Wrote the paper.

O.B. Adegbite: Performed the experiments.

N.O. Omisore: Performed the experiments; Wrote the paper.

Kayode Sanusi: Analyzed and interpreted the data; Wrote the paper.

Y. Yilmaz, Ü. Ceylan: Analyzed and interpreted the data; Contributed reagents, materials, analysis tools or data.

Funding statement

Craig Obafemi was supported by Central Science Laboratory, Obafemi Awolowo University.

Data availability statement

Data included in article/supplementary material/referenced in article.

Declaration of interests statement

The authors declare no conflict of interest.

Additional information

Supplementary content related to this article has been published online at https://doi.org/10.1016/j.heliyon.2020.e05756.

Acknowledgements

The support of the Central Science Laboratory (CSL), Obafemi Awolowo University, Ile-Ife, Nigeria is greatly acknowledged.

References

[1] A.K. Sen, S.B. Mahato, N.L. Dutta, Couroupitine A, a new alkaloid from *Couroupita guianensis*, Tetrahedron Lett. 15 (7) (1974) 609–610.
[2] J. Bergman, B. Egestad, J.O. Lindstroem, The structure of some indolic constituents in *Couroupita guaianesis* Abul.,, Tetrahedron Lett. 18 (30) (1977) 2625–2626.
[3] G. Honda, M. Tabata, Isolation of antifungal principle tryptanthrin, from *Strobilanthes cusia* O. Kuntze, Planta Med. 36 (1) (1979) 85–90.
[4] B.C. Liau, T.T. Jong, M.R. Lee, S.S. Chen, LC-APCI-MS method for detection and analysis of tryptanthrin, indigo, and indirubin in daqingye and banlangen, J. Pharm. Biomed. Anal. 43 (1) (2007) 346–351.
[5] G. Honda, V. Tosirisuk, M. Tabata, Isolation of an antidermatophytic, tryptanthrin, from indigo plants, *Polygonum tinctorium* and *Isatis tinctoria*, Planta Med. 38 (3) (1980) 275–276.
[6] T. Hashimoto, H. Aga, H. Chaen, S. Fukuda, M. Kurimoto, Isolation and identification of anti-Helicobacter pylori compounds from Polygonum tinctorium Lour, Nat. Med. (Tokyo) 53 (1999) 27–31.
[7] T. Mohn, I. Plitzko, M. Hamburger, A comprehensive metabolite profiling of *Isatis tinctoria* leaf extracts, Phytochemistry 70 (7) (2009) 924–934.
[8] V. George, A.S. Koshy, O.V. Singh, M.N.S. Nayar, P. Pushpangadan, Tryptanthrin from *Wrightia tinctoria*, Fitoterapia 67 (6) (1996) 553–554.
[9] M. Yoshikawa, T. Murakami, A. Kishi, T. Sakurama, H. Matsuda, M. Nomura, H. Matsuda, M. Kubo, Novel indole S,O-bisdesmoside, calanthoside, the precursor glycoside of tryptanthrin, indirubin, and isatin, with increasing skin blood flow promoting effects, from two *Calanthe* species (Orchidaceae), Chem. Pharm. Bull. 46 (5) (1998) 886–888.
[10] C.W. Jao, W.C. Lin, Y.T. Wu, P.L. Wu, Isolation, structure elucidation, and synthesis of cytotoxic tryptanthrin analogues from Phaius mishmensis, J. Nat. Prod. 71 (7) (2008) 1275–1279.
[11] Y.K. Lin, Y.L. Leu, T.H. Huang, Y.H. Wu, P.J. Chung, J.H. Su Pang, T.L. Hwang, Anti-inflammatory effects of the extract of indigo naturalis in human neutrophils, J. Ethnopharmacol. 125 (1) (2009) 51–58.
[12] F. Schindler, H. Zähner, Stoffwechselprodukte von Mikroorganismen 91. Mitteilung Tryptanthrin, ein von Tryptophan abzuleitendes Antibioticum aus Dandida Lipolytica, Arch. Microbiol. 79 (3) (1971) 187–203.
[13] I. Wagner-Döbler, H. Rheims, A. Felske, A. El-Ghezal, D. Flade-Schröder, H. Laatsch, S. Lang, R. Pukall, B.J. Tindall, Oceanibulbus indolifex gen. nov., sp. nov., a North Sea alphaproteobacterium that produces bioactive metabolites, Int. J. Syst. Evol. Microbiol. 54 (2004) 1177–1184.
[14] M.C. Recio, M. Cerdá-Nicolás, O. Potterat, M. Hamburger, J.L. Ríos, Anti-inflammatory and antiallergic activity in vivo of lipophilic Isatis tinctoria extracts and tryptanthrin, Planta Med. 72 (6) (2006) 539–546.
[15] K. Iwaki, E. Ohashi, N. Arai, K. Kohno, S. Ushio, M. Taniguchi, S. Fukuda, Tryptanthrin inhibits Th2 development, and IgE-mediated degranulation and IL-4 production by rat basophilic leukemia RBL-2H3 cells, J. Ethnopharmacol. 134 (2) (2011) 450–459.
[16] Y. Jahng, Progress in the studies on tryptanthrin, an alkaloid of history, Arch. Pharm. Res. 36 (5) (2013) 517–535.
[17] A.K. Bhattacharjee, D.J. Skanchy, B. Jennings, T.H. Hudson, J.J. Brendle, K.A. Werbovetz, Analysis of stereoelectronic properties, mechanism of action and pharmacophore of synthetic indolo[2,1-b]quinazoline-6,12-dione derivatives in relation to antileishmanial activity using quantum chemical, cyclic voltammetry and 3-D-QSAR CATALYST procedures, Bioorg. Med. Chem. 10 (6) (2002) 1979–1989.
[18] A.K. Bhattacharjee, M.G. Hartell, D.A. Nichols, R.P. Hicks, B. Stanton, J.E. van Hamont, W.K. Milhous, Structure-activity relationship study of antimalarial indolo [2,1-b]quinazoline-6,12-diones (tryptanthrins). Three dimensional pharmacophore modeling and identification of new antimalarial candidates, Eur. J. Med. Chem. 39 (1) (2004) 59–67.
[19] L.A. Onambele, H. Riepl, R. Fischer, G. Pradel, A. Prokop, M.N. Aminake, Synthesis and evaluation of the antiplasmodial activity of tryptanthrin derivatives, Int. J. Parasitol. Drugs Drug Resist. 5 (2) (2015) 48–57.
[20] G. Honda, M. Tabata, M. Tsuda, The antimicrobial specificity of tryptanthrin, Planta Med. 37 (2) (1979) 172–174.
[21] L.A. Mitscher, W. Baker, Tuberculosis: a search for novel therapy starting with natural products, Med. Res. Rev. 18 (6) (1998) 363–374.
[22] M. Kataoka, K. Hirata, T. Kunikata, S. Ushio, K. Iwaki, K. Ohashi, M. Ikeda, M. Kurimoto, Antibacterial action of tryptanthrin and kaempferol, isolated from the indigo plant (*Polygonum tinctorium* Lour.), against *Helicobacter pylori*-infected Mongolian gerbils, J. Gastroenterol. 36 (1) (2001) 5–9.
[23] J.M. Hwang, T. Oh, T. Kaneko, A.M. Upton, S.G. Franzblau, Z. Ma, S.N. Cho, P. Kim, Design, synthesis, and structure-activity relationship studies of tryptanthrins as antitubercular agents, J. Nat. Prod. 76 (3) (2013) 354–367.
[24] J. Scovill, E. Blank, M. Konnick, E. Nenortas, T. Shapiro, Antitrypanosomal activities of tryptanthrins, Antimicrob. Agents Chemother. 46 (3) (2002) 882–883.
[25] T. Kimoto, K. Hino, S. Koya-Miyata, Y. Yamamoto, M. Takeuchi, Y. Nishizaki, M.J. Micallef, S. Ushio, K. Iwaki, M. Ikeda, M. Kurimoto, Cell differentiation and apoptosis of monocytic and promyelocytic leukemia cells (U-937 and HL-60) by tryptanthrin, an active ingredient of *Polygonum tinctorium* Lour, Pathol. Int. 51 (5) (2001) 315–325.
[26] S.T. Yu, T.M. Chen, S.Y. Tseng, Y.H. Chen, Tryptanthrin inhibits MDR1 and reverses doxorubicin resistance in breast cancer cells, Biochem. Biophys. Res. Commun. 358 (1) (2007) 79–84.
[27] S.T. Yu, J.W. Chern, T.M. Chen, Y.F. Chiu, H.T. Chen, Y.H. Chen, Cytotoxicity and reversal of multidrug resistance by tryptanthrin-derived indoloquinazolines, Acta Pharmacol. Sin. 31 (2) (2010) 259–264.
[28] S. Yang, X. Li, F. Hu, Y. Li, Y. Yang, J. Yan, C. Kuang, Q. Yang, Discovery of tryptanthrin derivatives as potent inhibitors of indoleamine 2,3-dioxygenase with therapeutic activity in Lewis lung cancer (LLC) tumor-bearing mice, J. Med. Chem. 56 (21) (2013) 8321–8331.
[29] L.A. Mitscher, W.C. Wong, T. Demeulenaere, J. Sulko, S. Drake, Antimicrobial agents From higher plants. New synthesis and bioactivity of tryptanthrin (Indolo-[2,1-b]quinazolin-6,12-dione) and its analogues, Heterocycles 15 (2) (1981) 1017–1021.
[30] K.C. Jahng, S.I. Kim, D.H. Kim, C.S. Seo, J.-K. Son, S.H. Lee, E.S. Lee, Y. Jahng, One Pot synthesis of simple alkaloids: 2,3-polymethylene-4(3H)-quinazolinones, luotonin A, tryptanthrin, and rutaecarpine, Chem. Pharm. Bull. 56 (4) (2008) 607–609.
[31] J. Grimshaw, W.J. Begley, Synthesis of 2-anilino-3h-indol-3-one derivatives, Synthesis 7 (1974) 496–498.
[32] J. Bergman, J.O. Lindstroem, U. Tilstam, The structure and properties of some indolic constituents in *Couroupita guianensis* Aubl. Tetrahedron 41 (14) (1985) 2879–2881.
[33] T.V. Moskovkina, New synthesis of 6,12-dihydro-6,12-dioxoindolo[2,1-b] quinazoline (tryptanthrine, couropitine A), Russ. J. Org. Chem. 33 (1) (1997) 125–126.
[34] S. Eguchi, H. Takeuchi, Y. Matsushita, Short-step synthesis of rutecarpine and tryptanthrin via intramoleculer Aza-wittig reaction, Heterocycles 33 (1) (1992) 153–156.
[35] M. Matsui, M. Morita, K. Shibata, Y. Takase, Ozonolysis of Indigot, Nippon Kagaku Kaishi 1982 (7) (1982) 1268–1269.
[36] S.K. Pandey, Synthesis and evaluation of anti-inflammatory activity of 3-substituted indole derivative compound, J. Pharm. Res. 3 (11) (2010) 2738–2741.
[37] A. Subramoniam, D.A. Evans, S. Rajasekharan, G. Sreekandan Nair, Effect of hemigraphia colorata (Blume).{H}.{G}. Hallier on wound healing and inflammation in mice, Indian J. Pharmacol. 33 (2001) 283–285.
[38] R. Vinegar, J.F. Truax, J.L. Selph, F.A. Voelker, Pathway of onset, development and decay of carrageenan pleurisy in the rat, Fed. Proc. 41 (9) (1982) 2588–2595.
[39] B. Badilla, A.Y. Arias, M. Arias, G.A. Mora, L.J. Poveda, Anti-inflammatory and antinociceptive activities of Loasa speciosa in rats and mice, Fitoterapia 74 (1–2) (2003) 45–51.
[40] N.C. Staub, Pulmonary edema, Physiol. Rev. 54 (3) (1974) 678–811.
[41] E. Siegmund, R. Cadmus, G. Lu, A method for evaluating both non-narcotic and narcotic analgesics, Proc. Soc. Exp. Biol. Med. 95 (4) (1957) 729–731.
[42] O.O. Fadeyi, C.A. Obafemi, C.O. Adewunmi, E.O. Iwalewa, Antipyretic, analgesic, anti-inflammatory and cytotoxic effects of four derivatives of salicylic acid and anthranilic acid in mice and rats, Afr. J. Biotechnol 3 (8) (2004) 426–431.
[43] N.B. Eddy, D. Leimback, Synthetic analgesic. II. Dithienyl butenyl and dithienyl butylamines, J. Pharmacol. Exp. Ther. 107 (3) (1953) 385–393.
[44] O. Trott, A.J. Olson, AutoDock Vina: improving the speed and accuracy of docking with a new scoring function, efficient optimization and multithreading, J. Comput. Chem. 31 (2) (2010) 455–461.
[45] A.D. Becke, Density functional thermochemistry. III. The role of exact exchange, J. Chem. Phys. 98 (7) (1993) 5648–5653.
[46] M.J. Frisch, et al., Gaussian 03, Revision E.01, Gaussian, Inc., Wallingford CT, 2004.
[47] C.A. Obafemi, O.A. Fadare, J.P. Jasinski, S.P. Millikan, E.M. Obuotor, E.O. Iwalewa, S.O. Famuyiwa, K. Sanusi, Y. Yilmaz, Ü. Ceylan, Microwave-assisted synthesis, structural characterization, DFT studies, antibacterial and antioxidant activity of 2-methyl-4-oxo-1,2,3,4-tetrahydroquinazoline-2-carboxylic acid, J. Mol. Struct. 1155 (2018) 610–622.
[48] J.R. Cheeseman, G.W. Trucks, T.A. Keith, M.J. Frisch, A comparison of models for calculating nuclear magnetic resonance shielding tensors, J. Chem. Phys. 104 (14) (1996) 5497–5509.
[49] E. Cancès, B. Mennucci, J. Tomasi, A new integral equation formalism for the polarizable continuum model: Theoretical background and applications to isotropic and anisotropic dielectrics, J. Chem. Phys. 107 (8) (1997) 3032–3041.
[50] J. Tomasi, B. Mennucci, R. Cammi, Quantum mechanical continuum solvation models, Chem. Rev. 105 (8) (2005) 2999–3094.
[51] M. Namazian, P. Norouzi, R. Ranjbar, Prediction of electrode potentials of some quinone derivatives in acetonitrile, J. Mol. Struct. (Theochem) 625 (1–3) (2003) 235–241.
[52] M. Andoni, M. Medeleanu, M. Ştefănuţ, A. Căta, I. Ienaşcu, C. Tanasie, R. Pop, Theoretical determination of the redox electrode potential of cyanidin, J. Serb. Chem. Soc. 81 (2) (2016) 177–186.

[53] B.T. Psciuk, R.L. Lord, B.H. Munk, H.B. Schlegel, Theoretical determination of one-electron oxidation potentials for nucleic acid bases, J. Chem. Theory Comp. 8 (12) (2012) 5107–5123.

[54] S. Steenken, P. Neta, One-electron redox potentials of phenols. Hydroxy- and aminophenols and related compounds of biological interest, J. Phys. Chem. 86 (18) (1982) 3661–3667.

[55] R.S. Varma, Solvent-free organic syntheses on mineral supports using microwave irradiation, Clean Technol. Envir. 1 (2) (1999) 132–147.

[56] H.A. Ahangar, K. Marjani, G.H. Mahdavinia, Microwave-assisted reduction of α, β-unsaturated carbonyl compounds in solid state using sodium borohydide supported on magnesium sulfate ($NaBH_4/MgSO_4$-$7H_2O$), Synth. Commun. 38 (20) (2008) 3414–3421.

[57] Y. Torisawa, T. Nishi, J.I. Minamikawa, An efficient conversion of 5-nitroisatin into 5-nitroindole derivative, Bioorg. Med. Chem. Lett. 11 (6) (2001) 829–832.

[58] Y.M. Chung, J.M. Kim, J.N. Kim, Facile synthesis of 1-aryl-1, 2-ethanediols via the reduction of N-substituted isatins, Bull. Korean Chem. Soc. 24 (1) (2003) 141–143.

[59] J. Bergman, R. Carlsson, J.O. Lindstrom, The reaction of N-acetylisatin with hydroxylamine,, Tetrahedron Lett. 17 (40) (1976) 3611–3614.

[60] C.A. Obafemi, F.O. Taiwo, E.O. Iwalewa, D.A. Akinpelu, Synthesis, antibacterial and anti-inflammatory activities of some 2-phenylglyoxylic acid derivatives, Int. J. Life Sci. Pharma Res. 2 (2) (2012) 22–36.

[61] J.C. Maroon, J.W. Bost, A. Maroon, Natural anti-inflammatory agents for pain relief, Surg. Neurol. Int. 1 (2010) 80.

[62] J.W. Coleman, Nitric oxide in immunity and inflammation, Int. Immunopharmacol. 1 (8) (2001) 1397–1406.

[63] O. Werz, Inhibition of 5-lipoxygenase product synthesis by natural compounds of plant origin, Planta Med 73 (13) (2007) 1331–1357.

[64] K.I. Sengupta, K.V. Alluri, A.R. Satish, S. Mishra, T. Golakoti, K.V.S. Sarma, D. Dey, S.P. Raychaudhuri, A double blind, randomized, placebo controlled study of the efficacy and safety of 5-Loxin® for treatment of osteoarthritis of the knee, Arthritis Res. Ther. 10 (4) (2008) R85.

[65] T. Ishihara, K. Kohno, S. Ushio, K. Iwaki, M. Ikeda, M. Kurimoto, Tryptanthrin inhibits nitric oxide and prostaglandin E2 synthesis by murine macrophages, Eur. J. Parmacol. 407 (1–2) (2000) 197–204.

[66] Y. Takei, T. Kunikata, M. Aga, S. Inoue, S. Ushio, K. Iwaki, Tryptanthrin inhibits interferon-gamma production by Peyer's patch lymphocytes derived from mice that had been orally administered staphylococcal enterotoxin, Biol. Pharm. Bull. 26 (3) (2003) 365–367.

[67] R. Vinegar, W. Schreiber, R. Hugo, Biphasic development of carrageenin edema in Rats, J. Pharmacol. Exp. Ther. 166 (1) (1969) 96–103.

[68] P. Crunkhorn, S.C.R. Meacock, Mediators of inflammation induced in the rat paw by carrageenin, Br. J. Pharmacol. 42 (3) (1971) 392–402.

[69] B.G. Katzung, Basic and clinical pharmacology, 7th ed., Connecticut, Stanford, 1998, pp. 578–579.

[70] G.U. Rüster, B. Hoffmann, M. Hamburger, Inhibitory activity of indolin-2-one derivatives on compound 48/80-induced histamine release from mast cells, Pharmazie 59 (3) (2004) 236–237.

[71] Q. Feng, Y. Ren, Y. Wang, H. Ma, J. Xu, C. Zhou, Z. Yin, L. Luo, Anti-inflammatory effect of SQC-β-CD on lipopolysaccharide-induced acute lung injury, J. Ethnopharmacol. 118 (1) (2008) 51–58.

[72] C. Pergola, B. Jazzar, A. Rossi, H. Northoff, M. Hamburger, L. Sautebin, O. Werz, On the inhibition of 5-lipoxygenase product formation by tryptanthrin: mechanistic studies and efficacy in vivo, Br. J. Pharmacol. 165 (3) (2012) 765–776.

[73] Y.W. Kwon, S.Y. Cheon, S.Y. Park, J. Song, J.H. Lee, Tryptanthrin suppresses the activation of the LPS-treated BV2 microglial cell line via Nrf2/HO-1 antioxidant signaling, Front Cell Neurosci. 11 (2017) 18.

[74] A.L. Oaklander, Neuropathic itch, Semin. Cutan. Med. Surg. 30 (2) (2011) 87–92.

[75] A.L. Suárez, J.D. Feramisco, J. Koo, M. Steinhoff, Psychoneuroimmunology of psychological stress and atopic dermatitis: pathophysiologic and therapeutic updates, Acta Derm. Venereol. 92 (1) (2012) 7–15.

[76] R.G. Kurumbail, A.M. Stevens, J.K. Gierse, J.J. McDonald, R.A. Stegeman, J.Y. Pak, D. Gildehaus, J.M. Miyashiro, T.D. Penning, K. Seibert, P.C. Isakson, W.C. Stallings, Structural basis for selective inhibition of cyclooxygenase-2 by anti-inflammatory agents, Nature 384 (6610) (1996) 644–648.

[77] O. Llorens, J.J. Perez, A. Palomer, D. Mauleon, Structural basis of the dynamic mechanism of ligand binding to cyclooxygenase, Bioorg. Med. Chem. Lett. 9 (19) (1999) 2779–2784.

[78] L.J. Marnett, S.W. Rowlinson, D.C. Goodwin, A.S. Kalgutkar, C.A. Lanzo, Arachidonic acid oxygenation by COX-1 and COX-2. Mechanisms of catalysis and inhibition, J. Biol. Chem. 274 (33) (1999) 22903–22906.

[79] R.J. Terryn, H.W. German, T.M. Kummerer, R.R. Sinden, J.C. Baum, M.J. Novak, Novel computational study on π-stacking to understand mechanistic interactions of Tryptanthrin analogues with DNA, Toxicol. Mech. Methods 24 (1) (2014) 73–79.

[80] J.P. Mehta, P.H. Parmar, S.H. Vadia, M.K. Patel, C.B. Tripathi, In-vitro antioxidant and in-vivo anti-inflammatory activities of aerial parts of Cassia species, Arab. J. Chem. 10 (S2) (2017) S1654–S1662.

[81] W. Fedeli, F. Mazza, Crystal structure of tryptanthrin (indolo[2,1-*b*]quinazoline-6,12-dione), J. Chem. Soc. Perkin Trans. II 6 (13) (1974) 1621–1623.

[82] P.P. Bandekar, K.A. Roopnarine, V.J. Parekh, T.R. Mitchell, M.J. Novak, R.R. Sinden, Antimicrobial Activity of Tryptanthrins in *Escherichia coli*, J. Med. Chem. 53 (9) (2010) 3558–3565.

[83] Y.K. Al-Majedy, D.L. Al-Duhaidahawi, K.F. Al-Azawi, A.A. Al-Amiery, A.A.H. Kadhum, A.B. Mohamad, Coumarins as potential antioxidant agents complemented with suggested mechanisms and approved by molecular modeling studies, Molecules 21 (2) (2016) 135–145.

[84] H. Borsook, G. Keighley, Oxidation-reduction potential of ascorbic acid (vitamin C), Proc. Natl. Acad. Sci. U. S. A. 19 (9) (1933) 875–878.

[85] H. Danz, S. Stoyanova, P. Wippich, A. Brattström, M. Hamburger, Identification and isolation of the cyclooxygenase-2 inhibitory principle in *Isatis tinctoria*, Planta Med. 67 (5) (2001) 411–416.

[86] L. Doub, J.M. Vandenbelt, The ultraviolet absorption spectra of simple unsaturated compounds. I. Mono- and p-disubstituted benzene derivatives, J. Am. Chem. Soc. 69 (11) (1947) 2714–2723.

[87] H.E. Ungnade, The effect of solvents on the absorption spectra of aromatic compounds, J. Am. Chem. Soc. 75 (2) (1952) 432–434.

[88] L. Barros, S. Falcao, P. Baptista, C. Freire, M. Vilas-Boas, I.C.F.R. Ferreira, Antioxidant activity of *Agaricus* sp. mushrooms by chemical, biochemical and electrochemical assays, Food Chem. 111 (1) (2008) 61–66.

[89] R. Chang, Chemistry, 7th ed, McGraw-Hill, New York, NY, USA., 2001.